Int. J. Heat Mass Transfer. Vol. 15, pp. 935–952. Pergamon Press 1972. Printed in Great Britain

ELECTRIC FIELD INTENSITY AND WALL HEAT TRANSFER MEASUREMENTS FOR THE HEATING REGION OF AN ATMOSPHERIC CASCADE ARC

L. A. LUKENS and F. P. INCROPERA
Purdue University, West Lafayette, Indiana, U.S.A.

(*Received* 5 *May* 1971 *and in revised form* 17 *September* 1971)

Abstract—Electric field intensity and wall heat transfer measurements have been made for the inlet and asymptotic regions of Ar, He and N_2 laminar, atmospheric arcs. Comparisons between the data and available equilibrium and nonequilibrium theories have been made in an attempt to determine the relative accuracy of single and multifluid arc models. Equilibrium predictions for the asymptotic arc region in argon agree with the experimental results to within the combined experimental and theoretical uncertainties. There exist, however, small but discernable departures at both the lower and higher arc currents in argon. In contrast, the nonequilibrium theory predictions are in excellent agreement with the data over the entire range of currents. Additional comparisons suggest that atmospheric helium arcs are characterized by radical departures from local thermodynamic equilibrium.

NOMENCLATURE

- D, duct diameter;
- E, duct wall potential;
- E_x, electric field intensity;
- h, gas enthalpy, heat transfer conductance;
- I, arc current;
- k, thermal conductivity;
- k', translational thermal conductivity;
- k_{eff}, effective thermal conductivity ($k_{eff} = k' + \lambda_R$);
- L, total (cathode to anode) duct length;
- $\dot{m}$, operating gas flow rate;
- Nu, Nusselt number;
- Oh, Ohmic heating parameter;
- p, static pressure;
- P_R, radiation source density;
- q, total wall heat flux;
- $\bar{q}$, heat flux vector;
- q_{rad}, radiative wall heat flux;
- r, radial coordinate;
- R, duct radius;
- T, temperature;
- T_w, duct wall temperature;
- x, axial coordinate;
- Δx, duct segment width (= 0·632 cm);
- λ_R, reactive thermal conductivity;
- σ, electrical conductivity.

Subscripts

- a, asymptotic conditions;
- m, properties evaluated at the temperature corresponding to the mixed-mean enthalpy, h_m.

INTRODUCTION

In addition to serving as a reliable continuous energy source for transport and radiation property studies of high temperature gases, the electric arc has also served in technological applications which include industrial arc devices as well as thermonuclear fusion, MHD, and space propulsion systems. Accordingly, interest has evolved in the electrical and thermal characteristics of arc constrictors. The objective of this study is to enhance the understanding of these characteristics through an experimental investigation of electrical and thermal effects in an atmospheric cascade arc and through an interpretation of these effects in terms of available theories. While the major portion of the experimental work has been performed for an argon plasma, some measurements have also been made for nitrogen and helium arcs.

The regions of interest for the cascade arc are shown in Fig. 1. The arc column, which is a composite of individually water-cooled and electrically isolated copper discs, is divided into three regions: inlet, asymptotic, and anode.

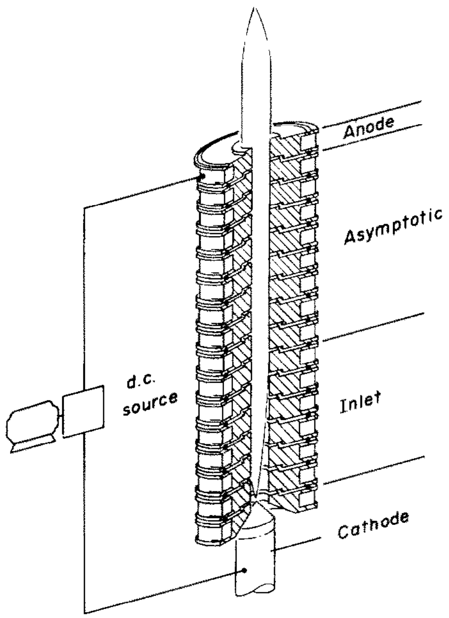

FIG. 1. Designation of arc-heating regions.

Although the gas flow in each region is subjected to an external electric field, the inlet and asymptotic regions are bounded by non-current-carrying surfaces, while the anode surface is electrically conducting. The inlet region is further distinguished by a significant axial variation of the flow variables, whereas the asymptotic region is characterized by thermally fully-developed flow.

Although the literature devoted to theoretical study of the inlet and asymptotic regions is extensive, few experimental studies have been performed for purposes of determining the overall arc energetics. Of particular scarcity are experimental studies pertaining to the inlet region of the water-cooled duct. Skifstad [1] performed electric potential and wall heat flux measurements in the inlet region of a helium arc, and investigators at the NASA-AMES Research Center [2–4] have made similar measurements in air and nitrogen arcs. However, the range of experimental conditions (gas flow rate, arc current, and duct geometry) investigated in these studies differ significantly from those of this investigation. Similarly, Pfender *et al.* [5] report results for the local wall heat flux in the inlet region of an argon cascade arc; however, these measurements were for turbulent flow and were used primarily for the support of anode heat transfer studies. In contrast, a larger number of experimental investigations have been performed for the asymptotic region of the arc [6–12]. While these studies are primarily concerned with the use of an inversion method to determine plasma transport properties, they necessarily include measurement of the arc-column electrical characteristics and are therefore germane to this study. In addition, Morris *et al.* [11] present asymptotic wall heat flux data and Emmons [10] and Maecker [12] report on the percentage contribution of radiation to the total energy balance.

Theoretical consideration of arc behavior has been extensive, and detailed reviews of work up to 1969 have been provided by Skifstad [13] and Bower [14]. Of the many theories, two in particular have been selected for consideration in this study. These include the approach by Stine and Watson [15], because of its inherent simplicity, and the treatment by Bower and Incropera [16], because of the completeness of the model and the attention given to the overall arc energetics. The Stine and Watson approach involves an approximate, analytical solution which ignores radiation and employs linearized property relations, whereas the Bower and Incropera approach involves numerical solution of a comprehensive flow model. Both theories have in common the assumption of local thermodynamic equilibrium.

Two other theories, which account for non-equilibrium effects and which have been chosen for consideration in this study, are those due to Pytte and Winsor [17] and Clark [18]. The Pytte and Winsor theory applies for the asymptotic region of a helium arc; however, the approach is semi-empirical due to its dependence on experimental arc-column characteristics. In addition, the theory suffers from the use of the Saha equation to compute the plasma composition. In contrast, Clark has formulated and numerically solved a complete multifluid model for the inlet and asymptotic regions of an arc constrictor.

The primary objective of this study is the measurement of the axial distribution of the electric field intensity, the mean enthalpy, and the heat flux for the inlet and asymptotic regions of an atmospheric Ar cascade arc. The measurements are made for a wide range of laminar flow operation conditions. An important secondary objective includes comparison of the asymptotic wall heat transfer and electric field strength measurements with various theoretical results. Attention is also given to ascertaining the validity of existing Nusselt number correlations and the adequacy of singlefluid models for the description of arc energetics. The measurements are also used to provide a greater understanding of the development length characteristics of the constricted tube, laminar arc. Additional experimental results are obtained for N_2 and He arcs to ascertain the influence of operating gas.

This study, which is the first serious attempt to experimentally varify existing theoretical predictions of thermal parameters for the arc heating region, is intended to provide information useful to the arc designer and to contribute to an improved understanding of arc physics and flow modeling.

EXPERIMENTAL APPARATUS AND INSTRUMENTATION

A well-defined, stable plasma flow is achieved through use of a constricted tube plasma arc generator manufactured by Creare, Inc. [19]. The constrictor is formed by stacking together a series of individually water-cooled copper segments, each of which is 0·632 cm wide with a 1·0 cm central bore. Each segment is electrically insulated from adjoining segments, and the length of the arc heating region may be varied according to the number of segments used to form the stack. A thoriated tungsten cathode is precisely centered with respect to the initial nozzle-shaped segment through micrometer adjustment, and the cathode-nozzle geometry provides for a high degree of flow symmetry.

Electrical power is supplied by a dc motor-generator set capable of delivering 75 kW at 300 A. Stable operating conditions are insured through use of a step-wise variable ballast resistor which is connected in series with the power supply and plasma generator. Cooling water is passed continuously through the cathode, each segment in the arc heating region, and the additional downstream ducting required to cool the gas for discharge. The coolant flow rate through each of these components may be independently controlled and monitored to within 1 per cent accuracy. The operating gas flow rate is also controlled and monitored to within 1 per cent accuracy. Stringent purity requirements are maintained throughout the gas system including use of research grade gas, prior ultrasonic cleaning of all components exposed to the plasma stream, and continuous outgassing of the system prior to operation. A detailed description of the plasma generator and supporting systems is provided by Lukens [20].

The overall and local electrical characteristics of the arc are determined by measuring the potential difference between the "floating" duct segments and the cathode. The arc voltage measurements are used to determine the axial distribution of the electric field intensity and, along with the arc current and calorimetric measurements, to determine the mixed-mean enthalpy of the gas at each segment location. The energy loss to each of the constrictor segments, to the cathode, and to the remaining plasma generator components is determined calorimetrically. Accordingly, each of these components is equipped with a special temperature difference (ΔT) transducer. Considerable care was taken in the shielding and calibration of the transducers, and they are accurate to within 5 per cent. The operating gas absolute temperatures at both inlet and discharge locations are measured with copper–constantan thermocouples.

A unique radiation gage is used to delineate the radiative contribution to the total wall heat flux. The gage consists of two semi-cylindrical copper segments which are thermally isolated from each other, individually water-cooled, and supplied with individual ΔT transducers. The inside (duct) wall of each half-segment is coated with either a highly reflecting (thermally evaporated aluminium film) or highly absorbing (black) surface. The overall dimensions of the radiation gage are precisely the same as those of a standard duct segment. A thorough discussion of the fabrication and principle of operation of the radiation gage is provided by Lukens [21].

A detailed uncertainty analysis is used to obtain the experimental uncertainty of each reported result. The method used in this analysis is the standard approach for single-sample experiments [22]. The uncertainty calculations, as well as the conversion and reduction of raw data, are performed on the computer. The thermophysical properties required for these calculations are obtained from Devoto [23] and Drellishak, Knopp and Cambel [24] for Ar; Lick and Emmons [25] and Devoto and Li [26] for He; and Drellishak, Aeschliman and Cambel [27] and Avco [28] for N_2.

To experimentally verify the accuracy of the diagnostic methods employed in this study, an attempt was made to "close off" the energy balance for the entire plasma generator. In all cases, it was possible to obtain closure to within the calculated total experimental uncertainty of this measurement (± 20 per cent). A more precise check is one based on a local energy balance performed on a segment located in the fully-developed portion of the arc heating region. In every case, closure of this local energy balance was obtained to within ± 5 per cent—a value comparable to the calculated uncertainty of these measurements. The consistent reproducibility of data taken over a 3-year period provided further confidence in the accuracy of the measurements and in the consistency of the overall system.

RESULTS

Experimental results are presented for Ar, N_2 and He arcs over the following ranges of laminar flow operating conditions:

Argon: $I = 35$–240 A, $\dot{m} = 0{\cdot}03$–$0{\cdot}11$ lb/min, constrictor length = 5 in. (20 segments)

Nitrogen: $I = 100$–200 A, $\dot{m} = 0{\cdot}03$ lb/min, constrictor length = 5 in. (20 segments)

Helium: $I = 50$ A, $\dot{m} = 0{\cdot}07$ lb/min, constrictor length = 2·5 in (10 segments).

All measurements were made with a 1·0 cm di. duct operating at atmospheric pressure. The maximum open-circuit voltage of the power supply, while adequate for obtaining a relatively wide range of Ar arc conditions, is insufficient to permit stable operation over as wide a range in N_2 and He.

Typical wall potential distributions are shown for an Ar arc in Fig. 2. For each distibution, the potential varies linearly with axial distance for entry lengths greater than 2·5 in. The 0·25 in. (1 segment length) location of the zero potential intercept is due to the positioning of the cathode within the initial nozzle-shaped segment. Potential distribution measurements were also made over the entire flow rate range, and although the potential at any location increased with $\dot{m}$, the slope of the distribution in the asymptotic region was independent of flow rate. The increase in the wall potential value at any axial location is due to the increase in the thermal development length with increasing $\dot{m}$. This results in a larger overall arc resistance;

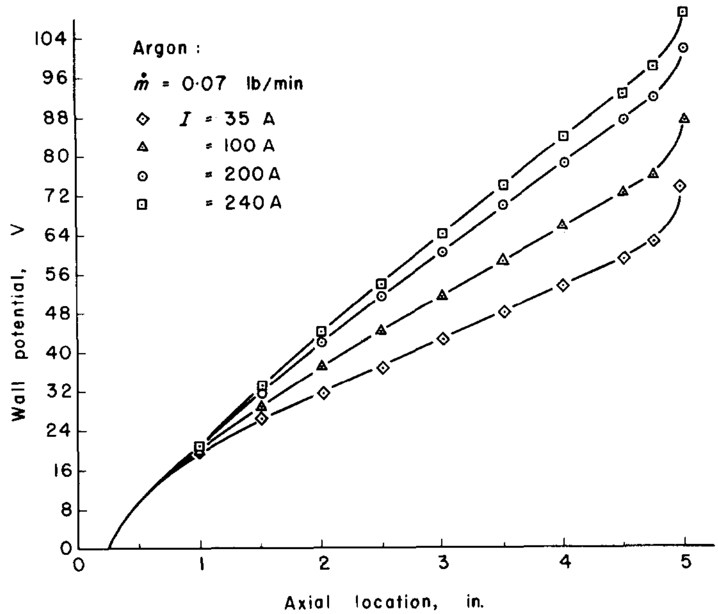

FIG. 2. Axial distribution of wall potential with arc current.

hence a larger potential must be applied to maintain a given current.

The asymptotic values of the electric field intensity for Ar, N_2 and He are plotted against arc current in Fig. 3. Included for comparison are the experimental distributions of Runstadler [7] and Emmons and Land [8] for Ar, Emmons [10] and McKee *et al.* [29] for He, and Emmons [10] for N_2. The excellent mutual agreement of results is apparent. While Emmons [10] contends that there are no regions (in a tube with $L/D = 14$) for which his N_2 data are independent

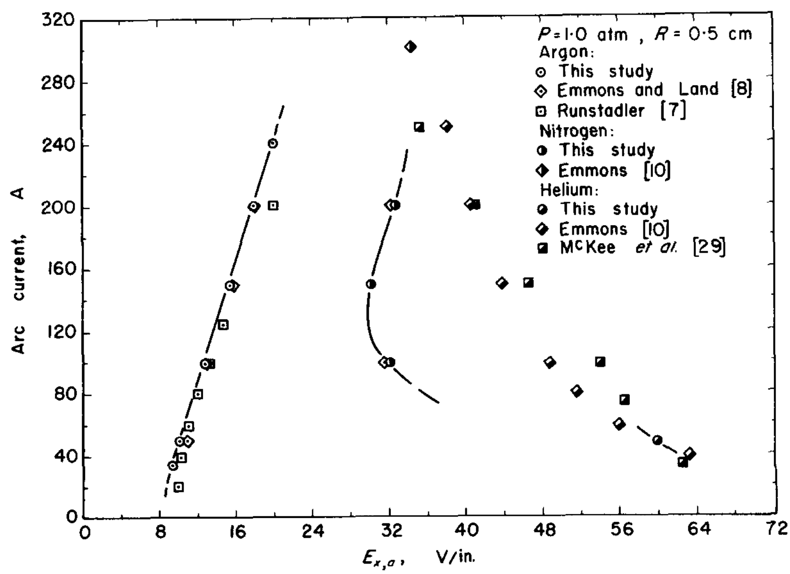

FIG. 3. Experimental asymptotic arc-column characteristics.

of laminar flow rate, asymptotic conditions (as evidenced by constant values of E_x and q in the axial direction) were observed in this study for $L/D \geqslant 12{\cdot}6$. Consequently, Emmons' lowest flow rate data were chosen as being the most representative of fully-developed flow.

Typical axial distributions of the total wall heat flux, q, and their variation with arc current in Ar are shown in Fig. 4. Similar distributions obtained for different values of $\dot{m}$ verify that q approaches a constant asymptotic value, q_a, which is independent of $\dot{m}$ [21]. The dependence of the asymptotic wall heat flux, q_a, on current is shown in Fig. 5 for the Ar, N_2 and He measurements of this study. Although the absence of similar data in the literature precludes a comparison with other investigatiors, confidence in the results may be established from a simple energy balance for the asymptotic region. For any segment in this region, the rate of energy removal through the tube wall must be balanced by the local input rate of electrical energy. Therefore,

$$q_a = \frac{E_{x,\,a} I}{2\pi R}. \tag{1}$$

The right-hand side of equation (1) was computed using the $E_{x,a}$-I data of Fig. 3 and the results are plotted for Ar in Fig. 5. The excellent agreement with the q_a results (determined calorimetrically) establishes confidence in the validity of these results. Moreover, this agreement provides a check on the overall self-consistency of the diagnostics, since closure of this local balance is obtained to within the combined experimental uncertainties of q_a (± 6 per cent), $E_{x,a}$ (± 3 per cent), and I (± 1 per cent).

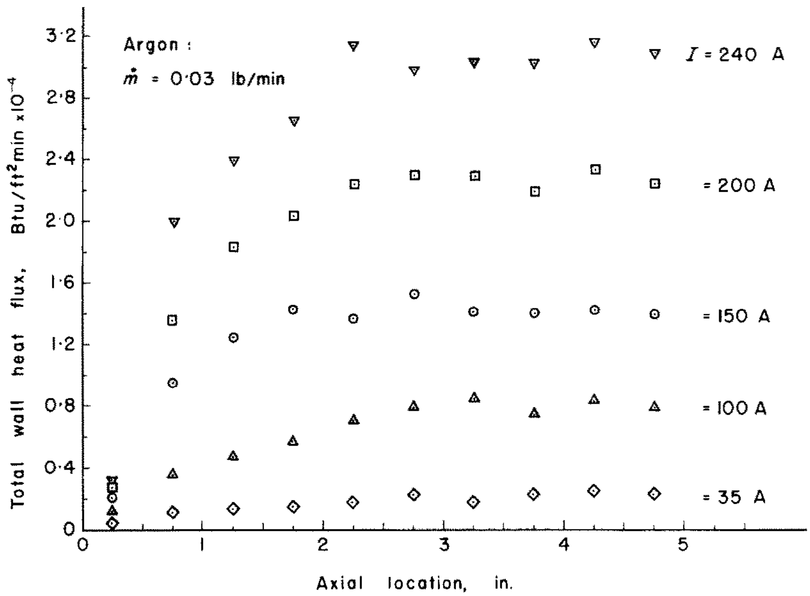

FIG. 4. Axial distribution of total wall heat flux with arc current.

The variation of the radiative wall heat flux for a fully-developed argon plasma with arc current is shown in Fig. 6. Also shown are the experimental data of Barzelay [30] and Emmons [9, 10]. The Harvard data are actually somewhat redundant in that the distribution reported by Emmons [10] was obtained by applying a correction factor of 1·5 to the data reported by Barzelay. In computing the electrical conductivity and radiation source strength properties for argon, Emmons determined that the correction factor was necessary in order to obtain the best fit to overall arc data. According to Fig. 6, however, better agreement exists between the

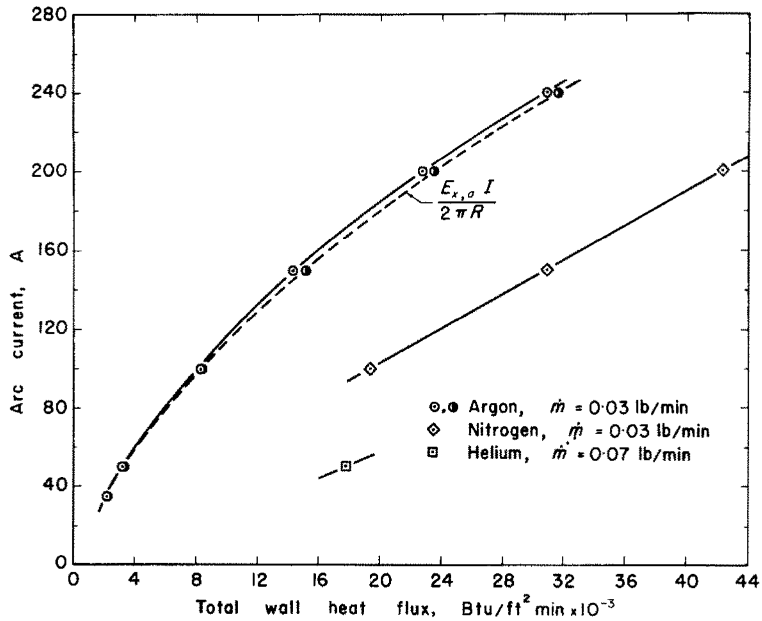

FIG. 5. Variation of the total wall heat flux with arc current in the asymptotic region.

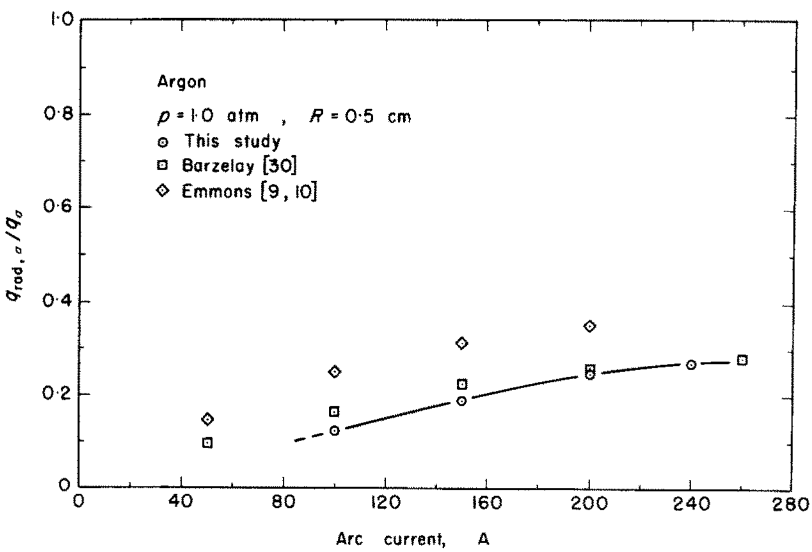

FIG. 6. Variation of the radiative wall heat flux with arc current in the asymptotic region of an argon plasma.

radiation data of this study and the original Harvard data reported by Barzelay.

Similarly, the axial distribution of the mixed-mean enthalpy (h_m) may be obtained by closing off the energy balance at successive axial locations. Under the assumption of thermodynamic equilibrium, the corresponding mean temperatures (T_m) may then be obtained from the caloric equation of state [24, 25, 27]. Such distributions also reflect an asymptotic condition, and the variations with arc current of $T_{m,a}$ in Ar, N_2 and He are shown in Fig. 7. Note the extremely low value of $T_{m,a}$ in He.

where k_m is chosen to be the thermal conductivity evaluated at the equilibrium temperature $T_{m,a}$ and T_w is the duct wall temperature (assumed constant at 500°K). Bower and Incropera [16] obtain a simple correlation of the Nusselt number in terms of an Ohmic heating parameter,

$$Oh_m \equiv \frac{R^2 \sigma_m k_m (T_{m,a} - T_w)}{I^2}, \tag{3}$$

which is of the form,

$$Nu_m = 0{\cdot}135(Oh_m)^{-1{\cdot}0}. \tag{4}$$

Although this correlation is inferred from parametric calculations involving the numerical

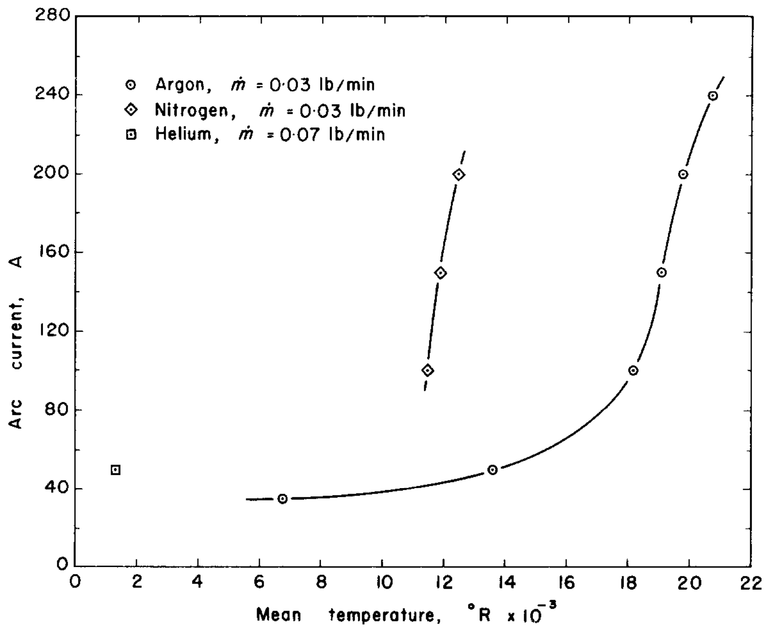

FIG. 7. Variation of the mean temperature with arc current in the asymptotic region.

The Nusselt number ($Nu = hD/k$) is introduced in an attempt to correlate, in terms of appropriate dimensionless parameters, the wall heat transfer in the asymptotic region of the laminar, constricted tube arc. By defining the heat transfer conductance (h) in terms of the total wall heat flux and a temperature potential, the Nusselt number takes the form

$$Nu_m = \frac{2Rq_a}{k_m(T_{m,a} - T_w)} \tag{2}$$

solution of an equilibrium flow model, a similar correlation of the form,

$$Nu_m = \frac{1}{\pi^2}(Oh_m)^{-1{\cdot}0} \tag{5}$$

may be obtained from simple order of magnitude arguments [21].

The above correlations are plotted in Fig. 8 along with the experimental results of this study for an Ar plasma. Although the comparison verifies the appropriateness of the Ohmic heating

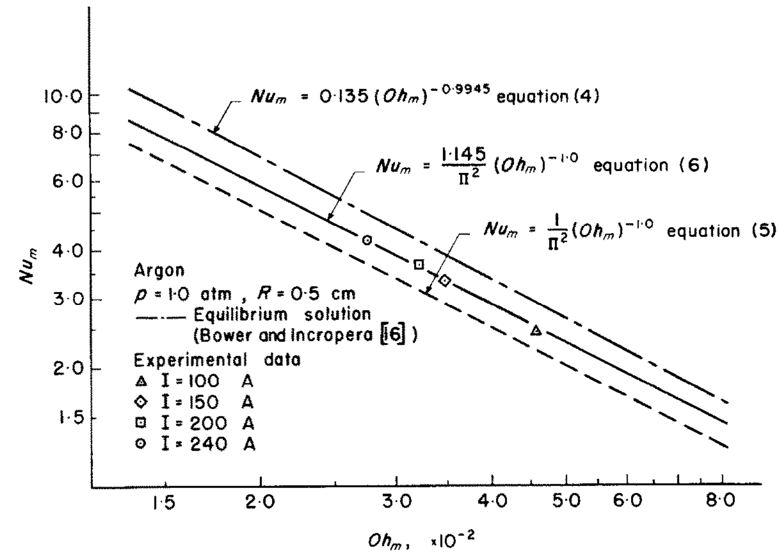

FIG. 8. Experimental and numerical Nusselt number correlations in the asymptotic region of an argon plasma.

parameter for arc heat transfer correlations, more precise corroboration is obtained from an empirical correlation of the form,

$$Nu_m = \frac{1.145}{\pi^2}(Oh_m)^{-1.0}. \tag{6}$$

It must be emphasized that the correlations summarized in Fig. 8 are only appropriate for an Ar plasma.

INTERPRETATION OF RESULTS AND COMPARISONS WITH THEORIES

The theoretical studies by Bower and Incropera [16] show that predictions for the inlet region of a constricted arc depend significantly upon the form of the assumed entrance profiles. Similarly, the results of this study show that measured quantities for the inlet region depend upon the position of the cathode relative to the the first segment. In contrast, both studies (theoretical and experimental) reveal no effect of entrance conditions on the properties of interest in the asymptotic region. Accordingly, meaningful comparisons between data and theory may only be made for this region.

Comparisons for argon are made between the experimental results of this study and the analytical solution by Stine and Watson [15], the numerical equilibrium solution by Bower and Incropera [16], and the numerical non-equilibrium solution by Clark [18]. Due to the scarcity of experimental data acquired in this study for helium, the experimental data of Emmons [10] are used for comparison with the theoretical results obtained by Bower [31], Pytte and Williams [32], and Pytte and Winsor [17]. For nitrogen, comparisons are made between the experimental results of this study and the Stine–Watson analytical solution. In making these comparisons, particular emphasis is placed upon ascertaining the influence of nonequilibrium effects on the arc parameters.

The experimental asymptotic values, for an Ar arc, of the electric field intensity ($E_{x,a}$), total wall heat flux, (q_a), and fraction of radiative to total wall heat flux ($q_{\mathrm{rad},a}/q_a$) are plotted as a function of arc current and compared with the aforementioned theories in Figs. 9–11, respectively. In all cases the agreement of the non-equilibrium predictions with data is excellent. The large disparities (in both magnitude and the functional dependence on arc current) between

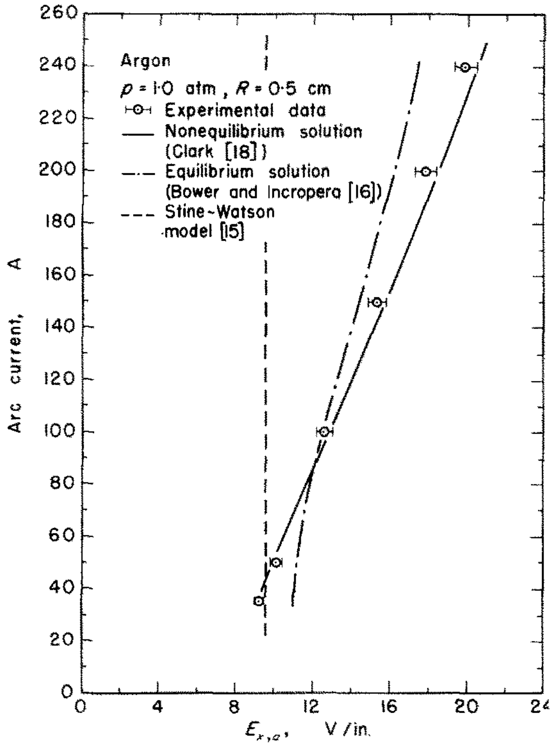

FIG. 9. Experimental and theoretical results for the asymptotic electric field intensity in argon.

the $E_{x,a}$ and q_a values obtained experimentally and those predicted from the simplified Stine–Watson model are thought to be due to two simplifications inherent in the model. These are the use of linearized property relations and the assumption of negligible radiation.

Comparison of the equilibrium numerical solution by Bower and Incropera and the data reveals excellent agreement in the 100 A range for both $E_{x,a}$ and q_a, while at lower and higher arc currents, respectively, the equilibrium theory overpredicts and underpredicts the data. In addition, although not shown on the figures, the deviations between the equilibrium and nonequilibrium predictions of $E_{x,a}$ and q_a continue to increase with increasing current above 240 A. Although the overall agreement is certainly adequate verification of the suitability of the equilibrium theory for engineering purposes and although any explanation of disparities must account for the effect of uncertainties in transport properties on the theoretical results, an explanation will nonetheless be attempted in terms of other considerations. Subsequent to

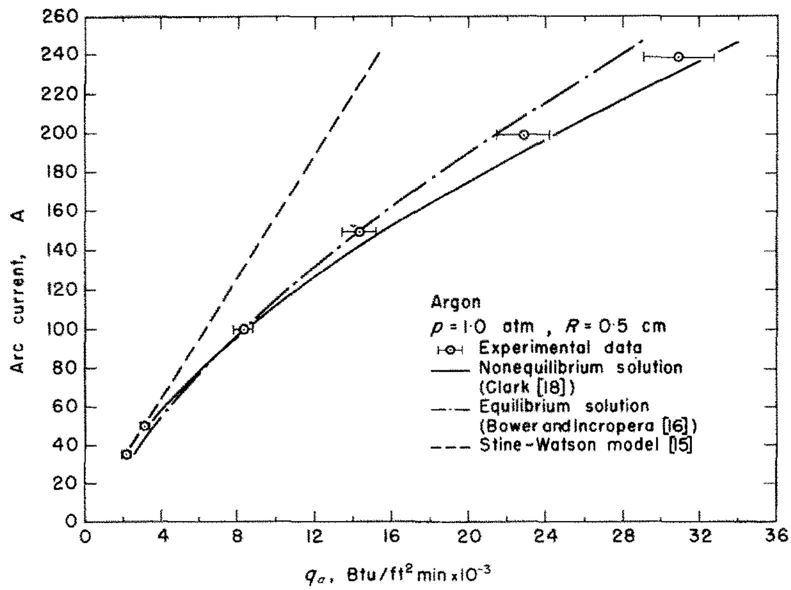

FIG. 10. Experimental and theoretical results for the asymptotic total wall heat flux in argon.

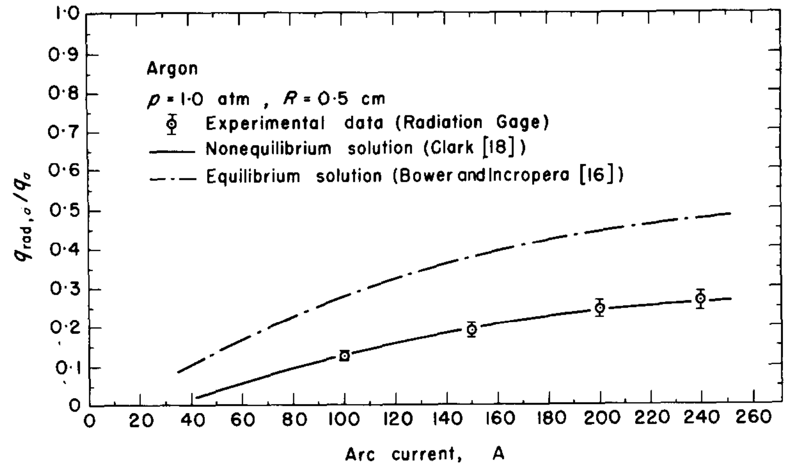

FIG. 11. Experimental and theoretical results for the fraction of radiative to total wall heat flux for the asymptotic region in argon.

this explanation, attention will be given to the influence of uncertainties in the transport properties.

A plausible explanation for the overprediction at the lower arc currents can be obtained from Ohm's law,

$$E_x = \frac{I}{2\pi \int_0^R \sigma r dr}. \tag{7}$$

If the low current arc experiences appreciable departures from equilibrium, the value of σ used in the equilibrium solution will be less than the actual value in those regions where non-equilibrium exists. Consequently, the theoretical evaluation of E_x through equation (7) will result in an overprediction of actual conditions. Likewise, through the requirement of equation (1) for the asymptotic region, an overprediction of q_a must result. Although this explanation suffices at low arc currents, it is not sufficient to explain the high current disparity.

Recent studies by Kruger [33], Incropera and Viegas [34], and Clark [18] indicate that in Ar nonequilibrium effects are most severe at low arc currents and diminish with increasing arc current. On this basis, the experimental results and equilibrium predictions which are compared in Figs. 9 and 10 should converge with increasing arc current when, in fact, they diverge for $I > 100$ A. Accordingly, the equilibrium underpredictions for $E_{x,a}$ and q_a at higher arc currents would not appear to be a result of wall-induced non-equilibrium.

A plausible explanation for the high current disparity is the inability of the equilibrium model to properly account for conduction effects at the elevated temperatures associated with high current operation. In particular, it is possible that the equilibrium model is underpredicting the energy transfer to the tube wall due to conduction. This contention is supported by the results of Fig. 11. Specifically, it is noted that, while excellent agreement exists between experiment and the nonequilibrium predictions for $q_{rad,a}/q_a$, the equilibrium prediction, for $I > 100$ A, is nearly double the nonequilibrium and experimental distributions. In comparing the equilibrium and nonequilibrium predictions for $q_{rad,a}/q_a$, it may be argued that the observed differences are the result of a dissimilarity in the radiation source density terms used in the two solutions. This is not the case, however, for it has been shown by Clark [18] that, in the limit of equilibrium, the radiation model employed in the nonequilibrium solution agrees favorably with the radiation source density used by Bower and Incropera and with experimental results [10]. The source density terms do not include the contributions of resonance radiation; hence the calculated radiation from the arc is not appreciably influenced by self-absorption effects. The overprediction of $q_{\mathrm{rad},a}/q_a$ is therefore most likely due to the higher temperature levels which characterize the equilibrium solution. This explanation is further supported by a comparison of values for the asymptotic mixed-mean enthalpy, $h_{m,a}$, obtained experimentally and from the equilibrium and nonequilibrium solutions. Although good agreement is obtained between the experimental and nonequilibrium theoretical results, the equilibrium theory consistently overpredicts the experimental results (a 40 per cent overprediction at 200 A) [21]. It is therefore felt that, for the higher arc currents in Ar, better agreement between experimental results and those obtained from the equilibrium theory could be achieved through a reduction of the equilibrium temperature profiles. This in turn could be achieved if the equilibrium model were to provide for greater energy loss by conduction.

In an effort to confirm the above premise, some attention was given to the thermal conductivity model of Devoto [23] which was employed in the equilibrium solution. In addition to the conventional translational mode of conduction, there is a transport of ionization energy through the ordinary diffusion of electron–ion pairs towards the outer regions of the arc. While the global conservation equations in the equilibrium model do not explicitly account for ordinary diffusion, an attempt is made to implicitly account for the resulting transport of ionization energy through the use of a reactive thermal conductivity, λ_R, which is defined by the heat flux vector expression [23]

$$\bar{q} \equiv -k'\nabla T - \lambda_R \nabla T. \tag{8}$$

On the basis of somewhat lengthy arguments [21], it was conclucded that the inability of the equilibrium model to provide for sufficient energy loss by conduction at higher arc currents is in large part due to its inability to properly account for the diffusion of ionization energy through the use of a reactive thermal conductivity.

Although attempts have been made to interpret Figs. 9–11 on the basis of nonequilibrium effects and thermal conductivity considerations, final judgement of the adequacy of the equilibrium model cannot be made until the combined experimental and theoretical uncertainties are considered. In an attempt to determine the range of uncertainties associated with the equilibrium solution, a parametric study was conducted [31] wherein the properties (σ, k_{eff}, and P_R) were selectively varied over their respective limits of estimated accuracy. The corresponding uncertainty band for the equilibrium heat flux prediction is shown in Fig. 12, along with the experimental data. On the basis of the overlap between the theoretical and experimental uncertainty bands, and in view of the previous discussion concerning the use of Devoto's formulation for the thermal conductivity, it is concluded that, to within the existing knowledge of plasma transport and radiation properties, singlefluid models are suitable for predicting asymptotic values for the total wall heat flux and the electric field intensity in argon, at least for arc currents up to 250 A. Conversely, the equilibrium model is not suitable for predicting $q_{\mathrm{rad},a}/q_a$ over the entire range of conditions investigated; nor is it adequate for predicting $h_{m,a}$ at the lower (<50 A) and higher (>150 A) arc current conditions [21]. In addition, it is felt that the equilibrium model would not be suitable for predicting $E_{x,a}$ and q_a if the above comparisons were extended to include conditions of lower and higher arc currents. In this respect, it is felt that a more rigorous theoretical treatment, such as the nonequilibrium solution by Clark [18], is required to accurately model the asymptotic region of the constricted tube argon arc.

Values of $E_{x,a}$ for helium obtained experimentally [10] and theoretically [17, 31, 32] are plotted in Fig. 13. Similarly, values of q_a for helium obtain experimentally at $I = 50$ A in this study and determined from the $E_{x,a}$ data of

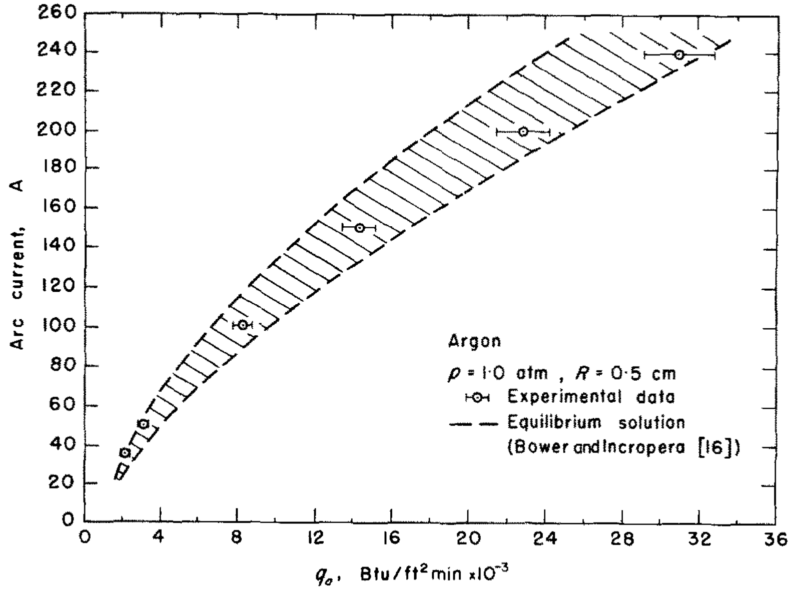

FIG. 12. The combined experimental and theoretical uncertainties for the asymptotic total wall heat flux in argon.

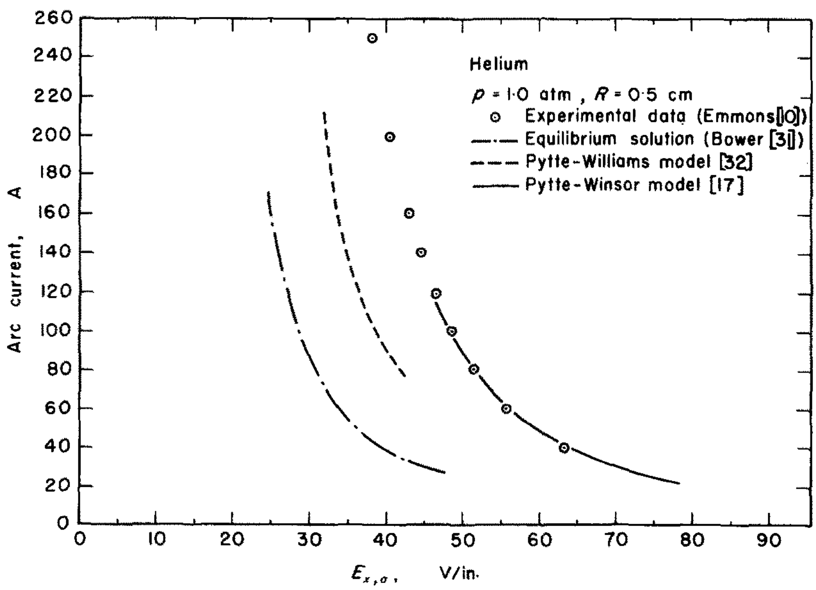

FIG. 13. Experimental and theoretical results for the asymptotic electric field intensity in helium.

[10] using equation (1) are plotted along with the equilibrium predictions of Bower [31] in Fig. 14. In comparing the equilibrium predictions with the experimental results, it is apparent that, unlike the previous comparisons for Ar, the singlefluid model is extremely deficient in describing the overall energetics of the helium arc. This deficiency is believed to be a result of the severe nonequilibrium conditions which are known to exist in low current ($I < 400$ A), atmospheric, helium arcs.

tion existed to sustain a luminescent arc. Such a result can only be indicative of a severe nonequilibrium condition in which free electrons at elevated kinetic temperatures coexist with heavy particles at low kinetic temperatures ($\sim$1000°R). For the same arc current, the equilibrium solution predicts a value of $T_{m,a} =$ 15700°R.

On the basis of these findings, it is felt that the comparisons between experiment and the equilibrium theory of Bower [31] are virtually

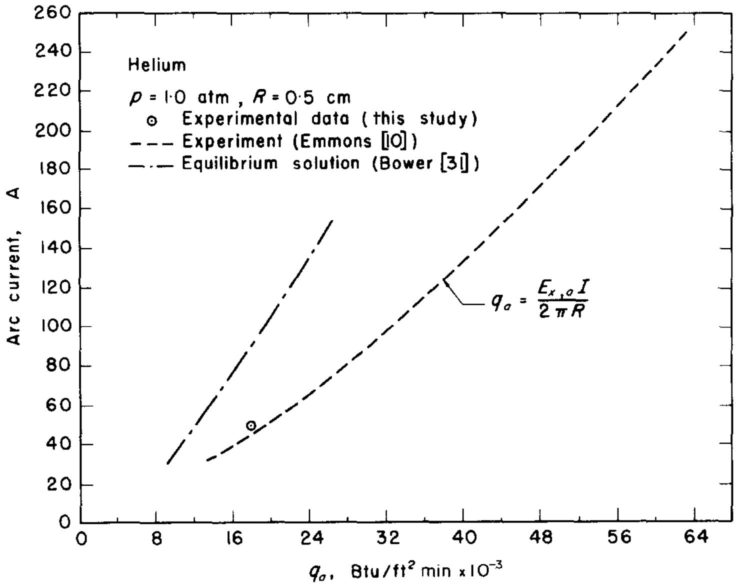

FIG. 14. Experimental and theoretical results for the asymptotic total wall heat flux in helium.

The pronounced departure of helium arc plasmas from local thermodynamic equilibrium has been observed and discussed by others, among the first of which were investigators at Harvard [9, 10, 35]. Further evidence of severe nonequilibrium conditions is provided by Kruger [33] and Aleksandrov [36] and by the data of this study. In addition, at an arc current of 50 A, measurements revealed a value of $T_{m,a} = 1350$°R (Fig. 7)* at the same time that sufficient ioniza-

meaningless. That is, since the plasma tube flow situation which the singlefluid model is attempting to describe bears little resemblance to the severe nonequilibrium state which actually exists, a systematic discussion of the differences is not possible. As shown in Fig. 13, the prediction of the arc-column characteristics in helium by Pytte and Williams [32] offers some improvement over the numerical solution by Bower; however, this theoretical model continues to underpredict $E_{x,a}$ by some 20 per cent. This underprediction by the Pytte–Williams model is attributed to the use of equilibrium calculations for σ and k [25] and to use of the Elenbaas–

* Note that, although the value of $T_{m,a}$ is based on equilibrium considerations, it provides a reasonable estimate of the heavy particle temperature for low degree of ionization.

Heller equation. Pytte and Winsor [17] have given greater consideration to nonequilibrium effects by proposing a two-temperature theory which accounts for thermal nonequilibrium between the electrons and heavy particles. However, the model suffers from use of equilibrium thermal conductivity values [25] and use of the Saha equation to determine the local composition. From the excellent agreement which exists between the Pytte–Winsor predictions and Emmons' experimental data for $E_{x,a}$, it would appear that use of the Saha equation and equilibrium thermal conductivities is justified. This agreement is misleading, however, for Pytte and Winsor adjusted their electrical conductivity in order to obtain the best fit to Emmons' arc-column data for $p = 1{\cdot}0$ atm and $R = 0{\cdot}5$ cm. In applying the resulting value of σ to calculations for tube radii other than $R = 0{\cdot}5$ cm, the model does predict the trends indicated by the experimentally determined shifts in the $E_{x,a}R$ vs. $E_{x,a}I$ curves; however, it fails to predict the magnitude of these shifts [17]. It is believed that this deficiency results from the failure of the Pytte–Winsor model to properly account for chemical nonequilibrium effects. Accordingly, the need remains for a rigorous, theoretical, multifluid model for the nonequilibrium flow of helium.

Similarly, the author knows of no multifluid analyses in the literature from which predictions of the global parameters, E_x and q, can be made for nitrogen arcs. Consequently, the following comparisons for nitrogen (Figs. 15 and 16) are limited to the singlefluid analytical model by Stine and Watson [15]. Relative to previous comparisons for argon, application of the Stine–Watson model to nitrogen provides better agreement with experiment. This is thought to be in part due to the lower temperature and radiation source levels which typify the nitrogen arc for a given current. As such, the negligible radiation assumption implicit in the Stine–Watson model would be less severe for nitrogen

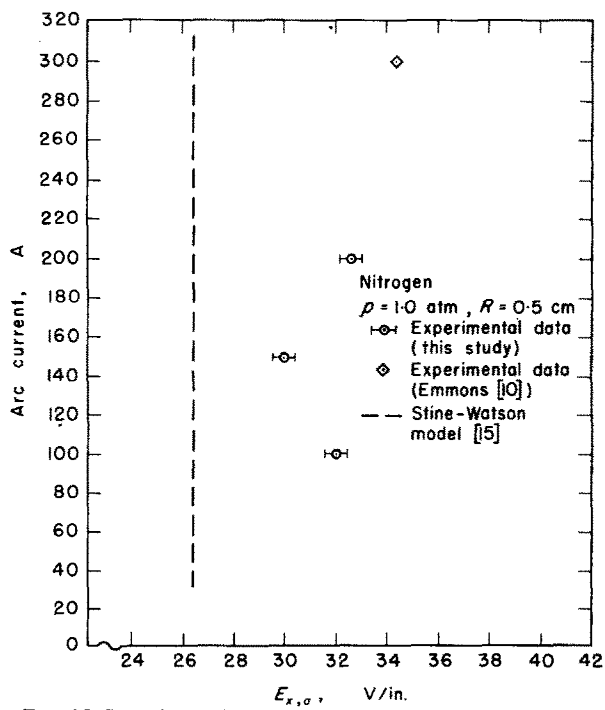

FIG. 15. Experimental and theoretical results for the asymptotic electric field intensity in nitrogen.

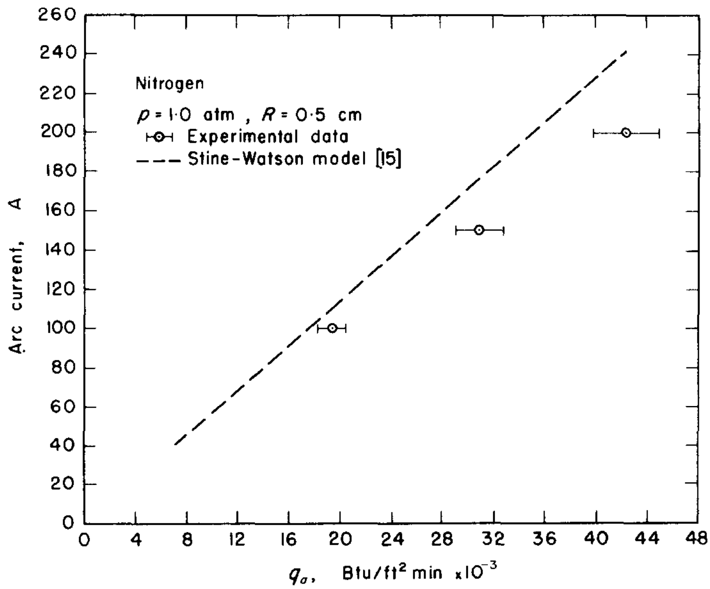

FIG. 16. Experimental and theoretical results for the asymptotic total wall heat flux in nitrogen.

than it is for Ar; nevertheless, as shown in Figs. 15 and 16, this assumption continues to render the model inaccurate at higher arc currents.

CONCLUSIONS

From the work of this study, the following conclusions are derived.

1. Variations in the duct entrance conditions can have a significant effect on the experimentally determined and numerically predicted electric field intensity and total wall heat flux distributions for the inlet regions of the constrictor. As a result, meaningful comparisons between experiment and theory can be made only for the asymptotic region.
2. Closed form analytical solutions which are based upon the use of linearized property relationships and which assume negligible radiation are inadequate for predicting electric field intensity and total wall heat flux. This is particularly evident at the higher current levels in argon and nitrogen.
3. To within the combined experimental and theoretical uncertainties (± 20 per cent), the numerical solution of a rigorous singlefluid model is suitable for use in predicting the electric field intensity and total wall heat flux for the asymptotic region in argon, at least over the range of conditions investigated in this study. The equilibrium solution does not, however, appear suitable for predicting the asymptotic temperature levels or the radiative wall heat flux over the same range of conditions in argon. There is a small, but discernible, nonequilibrium effect at the lower arc currents, as a result of which the equilibrium solution tends to overpredict both the electric field intensity and total wall heat flux. Moreover, the tendency of the equilibrium solution to underpredict these two parameters at arc currents in argon greater than 100 A is believed to be due to the failure of the equilibrium solution to provide for sufficient energy loss to the tube wall by conduction.
4. Solutions which properly account for thermochemical nonequilibrium, as well as for all pertinent transport phenomena, provide predictions for the electric field intensity and the convective and radiative wall heat transfer which are in excellent agreement with the

experimental results over the entire range of asymptotic conditions investigated in argon.

5. Atmospheric helium arcs are characterized by a significant departure from local thermodynamic equilibrium (at least for arc currents less than 250 A), and singlefluid models are totally inadequate for representing their thermal state.

REFERENCES

1. J. G. SKIFSTAD, Investigation of energy transfer in a tube arc heater, ARL 64-112 (1964).
2. C. E. SHEPARD and V. E. WATSON, Performance of a constricted-arc discharge in a supersonic nozzle, Fifth Gas Dynamics Symposium, Northwestern Univ. (1963).
3. H. A. STINE, V. E. WATSON and C. E. SHEPARD, Effect of axial flow on the behavior of the wall-constricted arc, AGARD-ograph 84, Part 1 (1964).
4. J. R. JEDLICKA and H. A. STINE, Axial flow through the wall constricted dc arc-comparison of theory and experiment, *IEEE Trans.* **NS-11**, 104–108 (1964).
5. E. PFENDER, G. D. RAITHBY and E. R. G. ECKERT, An anode comparison study in wall-stabilized argon arc, ARL 65-232 (1965).
6. H. MAECKER, Über die Charakteristiken zylindrischer Bogen, *Z. Phys.* **157**, 1–29 (1959).
7. P. W. RUNSTADLER, Laminar and turbulent flow of an argon arc plasma, Harvard Univ. Eng. Sci. Lab. T.R. 22 (1965).
8. H. W. EMMONS and R. I. LAND, Poiseulle plasma experiment, *Physics Fluids* **5**, 1489–1500 (1962).
9. H. W. EMMONS, Arc measurement of high temperature gas transport properties, *Physics Fluids* **10**, 1125–1136 (1967).
10. H. W. EMMONS, The arc measurement of high temperature gas transport properties, Harvard Univ. Eng. Sci. Lab. T.R. 23 (1965).
11. J. C. MORRIS, R. P. RUDIS and J. M. YOS, Measurement of electrical and thermal conductivity of hydrogen, nitrogen, and argon at high temperatures, *Physics Fluids* **13**, 608–617 (1970).
12. H. MAECKER, Transport properties in high power arcs, ARL 69-0031 (1969).
13. J. G. SKIFSTAD, Review of theoretical analyses of arc heating in a tube, ARL 65-207 (1965).
14. W. W. BOWER, Correlations for the wall parameters in the asymptotic region of a laminar constricted arc, M.S. Thesis, Purdue Univ. (1969).
15. H. A. STINE and V. R. WATSON, The theoretical enthalpy distribution of air in steady flow along the axis of a dc electric arc, NASA TN D-1331 (1962).
16. W. W. BOWER and F. P. INCROPERA, Heat transfer, development length, and friction factor correlations for the asymptotic region of a laminar arc constrictor, *Wärme und Stoffübertragung* **2**, 150–162 (1969).
17. A. PYTTE and N. K. WINSOR, A two-temperature theory for a helium arc plasma in a cylindrical duct, ARL 66-0047 (1966).
18. K. J. CLARK, Thermochemical nonequilibrium in an argon constricted arc plasma, HTGDL No. 4, School of Mech. Eng., Purdue Univ. (1971).
19. R. C. DEAN and P. W. RUNSTADLER, An arc plasma generator for research, AIAA Paper No. 66–162 (1966).
20. L. A. LUKENS, An experimental facility for heat transfer measurements in a high temperature plasma, M.S. Thesis, Purdue Univ. (1969).
21. L. A. LUKENS, An experimental investigation of electric field intensity and wall heat transfer for the heating region of a constricted arc plasma, Ph.D. Thesis, Purdue Univ. (1971).
22. S. J. KLINE and F. A. MCCLINTOCK, Describing uncertainties in single sample experiments, *Mech. Engng* **11**, 3–8 (1953).
23. R. S. DE VOTO, Transport coefficients of partially ionized argon, *Physics Fluids* **10**, 354–364 (1967).
24. K. S. DRELLISHAK, C. F. KNOPP and A. B. CAMBEL, Partition functions and thermodynamic properties of argon plasma, AEDC-TDR-68-146 (1963).
25. W. J. LICK and H. W. EMMONS, *Thermodynamic Properties of He to* 50,000°K. Harvard Univ. Press (1962).
26. R. S. DE VOTO and C. P. LI, Transport coefficients of partially ionized helium, *J. Plasma Phys.* **2**, 17–32 (1968).
27. K. S. DRELLISHAK, D. P. AESCHLIMAN and A. B. CAMBEL, Thermodynamic properties of argon, nitrogen, and oxygen plasmas, AEDC-TDR-64-12 (1964).
28. AVCO, Transport properties of nitrogen, hydrogen, oxygen, and air to 30,000°K, RAD-TM-63-7 (1963).
29. H. B. MCKEE, R. C. DEAN and A. PYTTE, On cooled anodes in contact with a laminar arc-heated flow, *IEEE Trans.* **NS-11**, 66–91 (1964).
30. M. E. BARZELAY, Thermal radiation from an argon plasma, Harvard Univ. Eng. Sci. Lab. T.R. 7 (1964).
31. W. W. BOWER, Private communication to L. A. LUKENS (1970).
32. A. PYTTE and A. R. WILLIAMS, On electrical conduction in a nonuniform helium plasma, ARL 63-166 (1963).
33. C. H. KRUGER, Nonequilibrium in confined arc plasmas, *Physics Fluids* **13**, 1737–1746 (1970).
34. F. P. INCROPERA and J. R. VIEGAS, Nonequilibrium in an arc constrictor, *AIAA Jl* **8**, 1772–1724 (1970).
35. J. F. BOTT, A spectroscopic investigation of a helium plasma arc, Harvard Univ. Eng. Sci. Lab. T.R. No. 25 (1966).
36. V. Y. ALEKSANDROV, D. B. GUREVICH and I. V. PODMOSHENSKII, Study of the mechanism of spectrum excitation in a helium arc plasma, *Opt. Spectrosc.* **26**, 18–20 (1969).

MESURES DE L'INTENSITÉ DU CHAMP ÉLECTRIQUE ET DU TRANSFERT PARIÉTAL THERMIQUE POUR LA RÉGION DE CHAUFFAGE D'UN ARC ATMOSPHÉRIQUE

Résumé—On a effectué des mesures d'intensité de champ électrique et de transfert thermique pariétal pour les régions internes et asymptotiques d'arcs atmosphériques laminaires de Ar, He et N_2. Des comparaisons entre les résultats et les théories utilisables d'équilibre et de non équilibre ont été faites pour essayer de déterminer la précision relative des modèles d'arc uniques ou multifluides. Des estimations de l'équilibre pour la région asymptotique d'arc dans l'argon s'accordent avec les résultats expérimentaux aux incertitudes expérimentales et théoriques près. Il existe cependant des écarts minimes mais discernables à la fois pour les courants d'arc les plus faibles et les plus élevés dans l'argon. Par contre, les estimations de la théorie de non équilibre sont en excellent accord avec les résultats sut tout le domaine de variation du courant. Des comparaisons additionnelles suggèrent que des arcs atmosphériques d'hélium sont caractérisés par de nets écarts à l'équilibre thermodynamique local.

MESSUNGEN DER ELEKTRISCHEN FELDSTÄRKE UND DES WANDWÄRMEÜBERGANGS FÜR DEN HEIZBEREICH EINES ATMOSPHÄRISCHEN KASKADENBOGENS

Zusammenfassung—Die elektrische Feldstärke und der Wandwärmeübergang wurden in den Einlass- und asymptotischen Bereichen von laminaren, atmosphärischen Ar-, He- und N_2-Bögen gemessen. Um die relative Genauigkeit von Einzel- und Vielfluid-bogenmodellen zu bestimmen, wurden die Ergebnisse mit erreichbaren Gleichgewichts- und Ungleichgewichts-Theorien verglichen. Gleichgewichtsvoraussagen für den asymptotischen Bogenbereich in Argon stimmen mit den experimentellen Ergebnissen innerhalb der kombinierten experimentellen und theoretischen Ungenauigkeit überein. Es gibt jedoch kleine aber wahrnehmbare Abweichungen sowohl bei kleineren als auch bei höheren Bogenströmen in Argon. Dagegen ergeben die Voraussagen der Nichtgleichgewichtstheorie ausgezeichnete Übereinstimmung mit den Ergebnissen über den ganzen Strombereich. Zusätzliche Vergleiche legen es nahe, dass atmosphärische Helium-bögen durch starke Abweichungen vom lokalen thermodynamischem Gleichgewicht charakterisiert sind.

ИЗМЕРЕНИЯ НАПРЯЖЕННОСТИ ЭЛЕКТРИЧЕСКОГО ПОЛЯ И ПЕРЕНОСА ТЕПЛА В ОБЛАСТИ НАГРЕТОГО УЧАСТКА ДУГО ПРИ АТМОСФЕРНОМ ДАВЛЕНИИ

Аннотация—Проводились измерения напряженности электрического поля и переноса тепла у стенки на ламинарных входном и асимптотическом участках дуг в аргоне, гелии и азоте в условиях атмосферного давления. Сравнивались экспериментальные и теоретические данные по равновесным и неравновесным состояниям с целью определения относительной точности простой и многокомпонентной моделей дуг. Равновесные расчеты в области асимптотического участка дуги в аргоне согласуются с экспериментальными данными с точность до некоторых экспериментальных и теоретических погрешностей. Однако существуют небольшие, но различимые отклонения как при низких, так и при высоких значениях тока длги в аргоне. Расчеты, выполненные по теории неравновесия, отлично согласуются с данными по всему диапазону изменения тока. Дополнительные сравнения позволяют сделать предположение, что дуги в гелии в условиях атмосферного давления характеризуются радикальными отклонениями от локадьного термодинамического равновесия.